International Journal of Coal Geology 81 (2010) 97–108

Contents lists available at ScienceDirect

International Journal of Coal Geology

journal homepage: www.elsevier.com/locate/ijcoalgeo

Impact of CO_2 injection and differential deformation on CO_2 injectivity under in-situ stress conditions

Zhongwei Chen [a], Jishan Liu [a,*], Derek Elsworth [b], Luke D. Connell [c], Zhejun Pan [c]

[a] School of Mechanical Engineering, The University of Western Australia, WA, 6009, Australia
[b] Department of Energy and Mineral Engineering, Penn State University, PA 16802-5000, USA
[c] CSIRO Petroleum Resources, Private Bag 10, Clayton South, Victoria 3169, Australia

ARTICLE INFO

Article history:
Received 2 September 2009
Received in revised form 22 November 2009
Accepted 23 November 2009
Available online 30 November 2009

Keywords:
CO_2 swelling
Coal permeability
Enhanced coalbed methane recovery
Numerical simulation

ABSTRACT

A fully coupled finite element (FE) model of coal deformation, gas flow and diffusion and competitive adsorption was developed to investigate the net effect on the evolution of CO_2 injectivity. Here we developed new cross coupling relations between coal porosity and mechanical, hydrological, binary gas diffusion and competitive adsorption-induced volumetric strains under variable stress conditions. The cubic relation between porosity and permeability is then applied to relate coal storage capability (changing porosity) to coal transport characteristics (changing permeability) also under variable stress conditions. These two relations coupled the multiphysics of coal–gas interactions. We implemented these two relations into a finite element model to represent the complex interactions of stress and gas composition under in-situ stress conditions. This relaxes the common assumption of prior studies that vertical stress remains constant and allows exploration of the full range of mechanical boundary conditions from invariant stress to restrained displacement. The FE model was verified against experimental data, and then extended to field scale to explore the sensitivity of CO_2 injection rate and ECBM production to in-situ stress conditions. Model results indicated that the net change in coal permeability accompanying binary gas diffusion is controlled competitively by the influence of effective stresses and differential matrix swelling. The balance between these two influences can be altered either by changing mechanical parameters (Young's modulus and Poisson's ratio) or by changing the coal sorption properties such as the swelling strain. The impact of gas sorption-induced deformation on coal permeability increases with the magnitudes of coal modulus or Poisson's ratio, and with the magnitudes of the gas swelling strain constant.

1. Introduction

CO_2-Enhanced Coalbed Methane (CO_2-ECBM) production involves the injection of CO_2 into a coal seam to promote the desorption of coalbed methane (CBM) while simultaneously sequestering CO_2 in the coal seam. This process exploits the greater affinity of carbon dioxide (CO_2) to adsorb onto coal relative to methane (CH_4), resulting in the net desorption of methane and its potential recovery as a low-carbon fuel. Laboratory isotherm measurements for pure gases have demonstrated that coal can adsorb approximately twice as much CO_2 (in mole) by volume as methane (White et al., 2005). Other laboratory experiments show that the ratio could be even larger at reservoir pressure higher than 9.6 MPa, where the gaseous CO_2 changes to supercritical CO_2 (Hall et al., 1994; Krooss et al., 2002). Recent research on the CO_2 sorption capacity of different ranks of United States coal has shown that this ratio may be as high as 10:1 in some low rank coals (Shi and Durucan, 2008). These observations are extremely important not only for CO_2 sequestration but also for coalbed methane production. Recent estimates of the worldwide coalbed CO_2 sequestration capacity are in the range 220 (Stevens et al., 1999) to 964 Gt (Kuuskraa and Boyer, 1992; Stauffer et al., 2009). Thus coalbeds represent significant potential sinks for anthropogenic CO_2, capable of accommodating ten to thirty five years of current emissions of almost 27 Gt per year (IPCC, 2005).

Since the concept of coal seam sequestration was first proposed by Macdonald of Alberta Energy during discussions with Gunter and coworkers in 1991(Gunter et al., 1997), a number of field CO_2-ECBM storage pilot projects have been undertaken in North America, Europe (Poland), China and Japan. The Allison Unit pilot, which is located in the Northern New Mexico part of the San Juan Basin, represents the world's first field trial of CO_2-ECBM in 1996 (Stevens et al., 1999). However, one of the technical obstacles faced in this technology is that the preferential sorption of CO_2 as CH_4 is desorbed can cause net swelling of the coal matrix (Levine, 1996; Pekot and Reeves, 2002; Chikatamarla et al., 2004). This excess dilatational strain in the coal matrix may competitively collapse the fracture porosity, resulting in

* Corresponding author.
E-mail address: jishan@cyllene.uwa.edu.au (J. Liu).

0166-5162/$ – see front matter © 2009 Elsevier B.V. All rights reserved.
doi:10.1016/j.coal.2009.11.009

net loss of permeability and reducing rates of CO_2 injection and CH_4 production (Fokker and van der Meer, 2004; Shi and Durucan, 2004). Injection rates in the Allison Unit pilot reduced by over 40% from an initial 141×10^3 m^3/day to only 85×10^3 m^3/day in the early stages of CO_2 injection. Similar dramatic reductions in CO_2 injectivity have also been observed in other field trials and confirmed in laboratory experiments (Krooss et al., 2002; Mazumder et al., 2005).

1.1. Experimental observations

The potential impacts of differential swelling on the performance and implementation of CO_2 geological sequestration projects have been investigated through experimental, field-scale, and numerical studies. Experiments on powdered high volatile bituminous Pennsylvanian coals have shown that adsorption rate decreases with increasing grain size for all experimental conditions (Busch et al., 2004). Similarly, coal type and rank (Robertson and Christiansen, 2005; Prusty, 2007) influences the preferential sorption behavior and the evolution of permeability with these changes linked to macromolecular structure (Mazumder and Wolf, 2007). The impacts of gas components on the efficiency of enhanced methane recovery are also investigated, indicating that the presence of the nitrogen component or flue gas in the injected gas stream is capable of improving the injectivity significantly (Durucan and Shi, 2008). Adsorption kinetics of CO_2 and CH_4 at different pressures and temperatures were experimented (Charrièrea et al., in press). Similarly, the sorption and swelling capacities of CO_2 under supercritical conditions were tested on various dry and water-containing coals with different pressures and temperatures (Siemons and Busch, 2007; Day et al., 2008). Distributed measurements of the sorption of CO_2 have shown temporal influences of diffusion into dual porosity media (Karacan, 2007) and the role of ambient stress in modulating swelling-induced strain (Pone et al., 2008).

1.2. Permeability and numerical models

Based on experimental observations, a variety of models have been formulated to quantify the evolution of permeability during coal swelling/shrinking. The first attempts to quantify the role of stresses on the evolution of coal-reservoir permeability assumed invariant vertical stresses and linked changes in horizontal stress with the gas pressure and the sorption strain (Gray, 1992). Permeability was computed as a function of reservoir pressure coal-matrix shrinkage assumed directly proportional to changes in the equivalent sorption pressure. Since then, a number of theoretical and empirical permeability models have been proposed. The Seidle-Huitt Model describes the evolution of permeability assuming that all changes in permeability are caused by the sorption-induced strain alone, neglecting the elastic strain (Seidle and Huitt, 1995). Another three of the most widely used permeability models are the Palmer and Mansoori model (P&M Model), the Shi and Durucan (S&D) model, and the Advanced Resources International (ARI) model (Palmer and Mansoori, 1996; Pekot and Reeves, 2002; Shi and Durucan, 2005). The P&M model is strain-based, which means porosity change is decided by the volume strain change, and the permeability change is calculated from porosity change. It is derived from an equation of linear elasticity for strain changes in porous rock assuming no change in overburden stress, that changes in porosity are small and that the permeating fluid is highly compressible. A cubic relationship between permeability and porosity is used to evaluate changes in permeability. The S&D model is based on an idealized bundled-matchstick geometry to represent a coalbed, and uses a stress-based formulation to correlate changes in the effective horizontal stress caused by the volumetric deformation together with the cleat or pore compressibilities. This stress-based model means porosity and permeability change does not come directly from volume strain change but via the horizontal stress change. Additionally, the Biot coefficient is set to unity — requiring that the change in net stress is equal to the difference between in overburden pressure and the change in pore pressure. The ARI model describes the evolution of coal permeability using a semi-empirical correlation to account for the changes of coal porosity due to pore compressibility and matrix swelling/shrinkage (Pekot and Reeves, 2002). ARI model is essentially equivalent to P&M model in saturated coal and where the strain versus stress fits the Langmuir isotherm (Palmer, 2009). More recently, an alternative approach has been proposed to develop an improved permeability model for CO_2-ECBM recovery and CO_2 geo-sequestration in coal seams, integrating the textural and mechanical properties to describe the anisotropy of gas permeability in coal reservoirs under confined stress conditions (Wang et al., 2009). However, although permeability models incorporating sorption-induced effects have been widely studied, these proposed studies are under the assumption of either an invariant total stress, or derived from the compressibility concept of porosity, which may provide incorrect outcomes or overestimates of permeability change (Pekot and Reeves, 2002; Robertson and Christiansen, 2007). These critical and limiting assumptions have been relaxed in new models rigorously incorporating in-situ stress conditions (Zhang et al., 2008) and are extended to rigorously incorporate CO_2–CH_4 coal–gas interactions relevant to CO_2-ECBM in this study.

Mechanical and permeability models incorporating the correct physics are essential for the accurate prediction of CO_2-ECBM recovery and CO_2 geosequestration through the use of upscaling numerical models. The effects of differential swelling on the feasibility of injection, capacity and security of long-terms storage is recognized as an important uncertainty for CO_2 injected into geologic (Pekot and Reeves, 2002; Korre et al., 2007; Stauffer et al., 2009). Additionally, the inclusion of varied sorption models including the Extended Langmuir model (ELM), the Ideal Adsorbed Solution (IAS) model and the Two-Dimensional Equation of State (2D EOS) model provide important constraints on rates and fluxes of gas uptake, and define rates of permeability change (Pan and Connell, 2009). These evolutions also include “weakening” and “plasticization” (Larsen, 2003) that may affect the evolution of the deformation modulus of coal over the extensive timescale of sequestration. Despite the complex models applied to represent the evolution of CO_2-ECBM reservoirs, few the mentioned models include feedbacks of both stress and CH_4–CO_2 counter-diffusion on the evolution of permeability. This latter effect of counter-diffusion is significant as CO_2 replaces CH_4. This effect may be incorporated through multicomponent gas diffusion and flow in bulk coals such as the bidisperse diffusion using Maxwell–Stefan (MS) diffusion (Wei et al., 2007). This behavior has been further explored for a multi-continuum porous medium with triple porosity and dual permeability, focusing on mass exchange and the interaction of micropores, marcopores and fractures (Fathi and Akkutlu, 2008; Yi et al., 2008) but for invariant permeability and diffusivity due to stress effects. Finally, the roles of deformation and flow with two components have been investigated (Connell and Detournay, 2009). Similar numerical models have been used to investigate CO_2 injectivity, one of the most important parameters for CO_2 sequestration, including the co-injection of nitrogen to delay or suppress influences of CO_2-induced swelling (Shi and Durucan, 2004; Durucan and Shi, 2008). The presence of nitrogen was shown capable of improving the efficiency of gas injection significantly over pure CO_2 injection with matrix and fracture permeability and the cleat system porosity as the most sensitive parameters (Fokker and van der Meer, 2004).

1.3. Proposed study

Experimental, theoretical and field observations, as presented above, have illustrated that the injection of CO_2 into coal seams

triggers complex interactions of stress and chemistry. These interactions have a strong influence on the properties of coal. These include influences on gas sorption and flow, coal deformation, porosity change and permeability modification. Although coal–gas interactions have been comprehensively investigated, most of these prior studies focus on one or more individual processes under special conditions. For those studies on interactions of stress and chemistry, they usually assume that these interactions are under conditions of invariant total stress where effective stresses scale inversely with applied pore pressures. In this study, we define the chain of coal–gas interactions as "coupled multiphysics" implying that one physical process affects the initiation and progress of another. The individual processes, in the absence of full consideration of cross couplings, form the basis of very well-known disciplines such as adsorption, elasticity, and gas transport. Therefore, the inclusion of cross couplings is the key to rigorously formulate the coupled multiphysics of coal–gas interactions. Here we develop new cross coupling relations between coal porosity and mechanical, hydrological, and binary gas diffusion and competitive adsorption induced volumetric strains under conditions of variable stress. The cubic relation between porosity and permeability is then introduced to relate coal storage capability (changing porosity) to coal transport characteristics (changing permeability) also under variable stress conditions. These two relations are the key cross couplings that couple the multiphysics of coal–gas interactions. We implement these two relations into a finite element model to represent the complex interactions of stress and chemistry under in-situ conditions. This relaxes the prior assumption that total stresses remain constant and allows exploration of the full range of mechanical boundary conditions from invariant stress to restrained displacement.

2. Governing equations

A model is developed to represent the effects of stress and mechanical restraint on the evolution of porosity and permeability in a porous medium. The following assumptions are considered in the modeling:

(a) Coal is a homogeneous, isotropic and elastic continuum, and the system is isothermal.
(b) Strains are infinitesimal.
(c) Gas contained within the pores is ideal, and its viscosity is constant under isothermal conditions.
(d) Gas flow through the coal matrix is assumed to be viscous flow obeying Darcy's law (a water phase is not included in the model).

2.1. Gas adsorption/desorption and induced strain

Henry's Law (1803) (e.g. King, 1990), an equilibrium adsorption isotherm, describes a relationship between the adsorbed (V) and free gas (C) concentrations as:

$$V = f(C, a, b) \tag{1}$$

where a and b are model parameters. The linear Henry's law isotherm is the simplest possible model defining a constant ratio between the adsorbed gas and free gas concentrations. However, this simple form is rarely used in coals since at typical gas pressures of interest the sorbed mass is limited to a threshold capacity — typically interpreted as a limitation in the number of available sorption sites. The Langmuir isotherm accommodates this important feature with an upper limit in sorbed mass and is defined as (Langmuir, 1916):

$$V = \frac{V_0 aC}{1 + aC}. \tag{2}$$

In this a is the Langmuir equilibrium constant, which describes the partitioning of adsorbate molecules between the adsorption sites and the free unassociated state and V_0 represents the maximum number of sites available for the adsorbing molecules (adsorption capacity). This relation is derived from both kinetic and statistical mechanical points of view. The mechanism described in the Langmuir model is the adsorption of adsorbate molecules on a fixed number of well-defined localized sites, each of which can hold only one adsorbate molecule. All sites are energetically equivalent and there is no interaction between adsorbate molecules adsorbed on neighboring sites (Fathi and Akkutlu, 2009). Although alternate expressions have been proposed, some based on pore filling theory (e.g. the Dubinin-Astakhov equation) (Dubinin, 1966), the Langmuir adsorption isotherm remains most widely used due to its simplicity and its accord with wide-ranging experimental data (Chaback et al., 1996).

The prior cases relate to a single gas system but the gas adsorbed on coal is not always pure methane. Coal can also adsorb appreciable amounts of CO_2, N_2 and hydrocarbons (e.g. ethane and propane) with these multiple compete competing for a finite number of sorption sites. Due to this competition, the sorption of each component is less than when both gases act independently. In these cases, a multi-component gas sorption isotherm is needed in order to predict the composition of the produced gas, the reserve of Gas-In-Place and rates of recovery, especially for primary recovery by pressure depletion and for secondary recovery by CO_2 injection. Among existing methods the Extended Langmuir Isotherm (ELI) is a straightforward and relative accurate method of representing multi-component adsorption behavior.

The ELI is expressed as:

$$V_k = \frac{V_{k0} C_k b'_k}{1 + \sum_{j=1}^{N} C_j b'_j} \tag{3}$$

where subscripts i and j refer to the gas components, C_k is the concentration of gas component k, N is the number of gas components and b'_j is the Langmuir pressure constant for gas j.

For a binary mixture of CH_4 (component 1) and CO_2 (component 2), the total amount of gas adsorbed on the coal at any given pressure is given by:

$$V_t = \sum_{k=1}^{2} V_k = \frac{V_{10} C_1 b'_1 + V_{20} C_2 b'_2}{1 + C_1 b'_1 + C_2 b'_2}. \tag{4}$$

The values of V_{10} and V_{20} are initially known as they represent the gas adsorption capacity for each component and can be determined by isotherm measurement.

Volume changes in coal are known to accompany gas sorption and desorption (Moffat and Weale, 1955). Experimental sorption-induced strain data from recent studies (Levine, 1996; Chikatamarla et al., 2004; Cui and Bustin, 2005) indicate that the gas sorption-induced volumetric strain is approximately proportional to the volume of gas adsorbate, irrespective of its mixed composition. Thus the volume strain may be defined as

$$\varepsilon_k = \varepsilon_g \cdot V_k = \varepsilon_{\infty k} \frac{aC}{1 + aC} \tag{5}$$

where ε_g is the sorption-induced strain coefficient to gas sorption volume, $\varepsilon_{\infty k} = \varepsilon_g \cdot V_{k0}$ is the gas swelling strain constant.

The advantage of using a linear function is that obtaining precise volumetric strain data is difficult because of the complexity of the experiments, and so far, volumetric strain experiments have been conducted on very few coals. Thus, the sorption-related volumetric strain accompanying gas production for different coals can be readily modeled even if only the isotherm is known. In this model, it is presumed that the gas sorption-induced strain ε_k is to result in

volumetric strain only. Its effects on all three normal components of strain are identical as evident in laboratory observations (Levine, 1996; Robertson and Christiansen, 2005).

Experimental evidence (Butler and Ockrent, 1930; Do, 1998) supports the use of the extended Langmuir isotherm equation in representing the adsorption of gas mixtures. By analogy with this equation for gas mixture adsorption, the volumetric strain caused by sorption at any composition and pressure due to each gas species can be computed as

$$\varepsilon_k = \varepsilon_{\infty k} \frac{C_k b'_k}{1 + \sum_{j=1}^{N} C_j b'_j}. \tag{6}$$

The total sorption-induced strain is determined by summing the strains caused by each gas species, as,

$$\varepsilon_s = \sum_{k=1}^{n} \varepsilon_k \tag{7}$$

where ε_s is the total sorption-induced strain, b'_k represents the Langmuir pressure constant for component k, $\varepsilon_{\infty k}$ represents the gas volumetric strain of component k at infinite pressure and C_k is the concentration of gas component k.

2.2. Coal deformation

The deformation of the coal matrix is affected by gas absorption/desorption, gas flow and transport and initial and boundary conditions. The coal matrix shrinks when CH_4 desorbs from coal matrix and it swells when CO_2 absorbs to the coal matrix. Injection of gas in a network of natural fractures initiates transport and competitive (and often selective) sorption and transport processes among the gas molecules in coal. Consequently, the incoming CO_2 molecules activate and displace the in-place CH_4 molecules. Gas transport and exchange typically causes significant changes in effective stress, which then influence coal matrix deformation and the evolution of transport parameters.

Coal deformation is defined through the Navier equation for linear poroelastic media, accommodating pore pressure and absorption/desorption induced effects as additional source terms acting as additional body forces. According to assumption (a), the strain-displacement relation is defined as

$$\varepsilon_{ij} = \frac{1}{2}(u_{i,j} + u_{j,i}) \tag{8}$$

and the equilibrium equation is defined as

$$\sigma_{ij,j} + f_i = 0 \tag{9}$$

where ε_{ij} is the component of the total strain tensor, u_i is the component of the displacement, σ_{ij} denotes the component of the total stress tensor and f_i denotes the component of the body force. Accommodating the influences of pore pressure and sorption-induced strain (Detournay and Cheng, 1993; Zhang et al., 2008), the constitutive relation for the deformed coal seam becomes

$$\varepsilon_{ij} = \frac{1}{2G}\sigma_{ij} - \left(\frac{1}{6G} - \frac{1}{9K}\right)\sigma_{kk}\delta_{ij} + \frac{\alpha}{3K}p\delta_{ij} + \frac{\varepsilon_s}{3}\delta_{ij} \tag{10}$$

where $G = \frac{E}{2(1+\nu)}$, $K = \frac{E}{3(1-2\nu)}$. K and K_s represent the bulk modulus of coal and coal grains respectively, G is the shear modulus of coal, E is the Young's modulus of coal, ν is the Poisson ratio of coal, and δ_{ij} is the Kronecker delta.

According to the equation of state (EOS) for the binary gas, each partial pressure (p_k) and the total pressure (p) for the binary flow system can be expressed as

$$p_k = C_k \cdot RT \cdot z_k \tag{11}$$

$$p = \sum_{k=1}^{2} C_k \cdot RT \cdot z_k \tag{12}$$

where z_k is the correction factor that accounts for the non-ideal behavior of the gas which changes with pressure and temperature and R and T represent the universal gas constant and absolute temperature.

To simplify the treatment here, both gases are considered as ideal ($z_k = 1$), so the effective stress σ_{eij} can be defined as:

$$\sigma_{eij} = \sigma_{ij} + \alpha \cdot \sum_{k=1}^{2} C_k \cdot RT \cdot \delta_{ij}. \tag{13}$$

Combining Eqs. (8)–(13) yields the Navier-type equation expressed as

$$Gu_{i,kk} + \frac{G}{1-2\nu}u_{k,ki} = (\alpha \cdot RT + K \cdot AA)C_{1,i} + (\alpha \cdot RT + K \cdot BB)C_{2,i} - f_i \tag{14}$$

where $AA = \frac{\varepsilon_{\infty 1} b'_1 (1 + b'_2 C_2)}{(1 + C_1 b'_1 + C_2 b'_2)^2} - \frac{\varepsilon_{\infty 2} b'_1 b'_2 C_2}{(1 + C_1 b'_1 + C_2 b'_2)^2}$, $BB = \frac{\varepsilon_{\infty 2} b'_2 (1 + b'_1 C_1)}{(1 + C_1 b'_1 + C_2 b'_2)^2} - \frac{\varepsilon_{\infty 1} b'_1 b'_2 C_1}{(1 + C1 b'_1 + C_2 b'_2)^2}$.

Both terms on the left side of Eq. (14) represent the elastic deformation of the system influenced by equivalent fluid pressure and sorption-induced body forces. The first and third terms on the right side of Eq. (14) represent the effects of pore pressure; the second and fourth terms on the right side reflect the influence of gas absorption on coal deformation and the fifth term represents a generic body force within the porous medium system, typically accommodating self-weight of the medium.

2.3. Permeability evolution model

As discussed in Section 2.1, the sorption-induced volumetric strain for gas mixtures can be represented by the extended Langmuir isotherm equation. By analogy with the porosity and permeability equations for single gas flow, the relationships can be extended to multi-components gas transport system.

In this paper, the following equation is chosen to calculate the relation between permeability and porosity

$$\frac{k}{k_0} = \left(\frac{\phi}{\phi_0}\right)^3 \tag{15}$$

Considering a porous medium containing solid volume of V_s and pore volume of V_p, we assume the bulk volume $V = V_p + V_s$ and the porosity $\phi = V_p/V$. From Eq. (10), we obtain that

$$\varepsilon_v = -\frac{1}{K}(\overline{\sigma} - \alpha \cdot \sum_{k=1}^{2} C_k \cdot RT \cdot z_k) + \varepsilon_s \tag{16}$$

According to Eq. (16), the volumetric evolution of the porous medium can be described in terms of $\Delta V/V$ and $\Delta V_p/V_p$, the volumetric strain of coal and volumetric strain of pore space, respectively. The relations are

$$\frac{\Delta V}{V} = -\frac{1}{K}(\Delta\overline{\sigma} - \alpha \cdot \Delta p) + \Delta\varepsilon_s \tag{17}$$

$$\frac{\Delta V_p}{V_p} = -\frac{1}{K_p}(\Delta\overline{\sigma} - \beta\cdot\Delta p) + \Delta\varepsilon_s \tag{18}$$

where α is the Biot coefficient, $\alpha = 1 - K/K_s$, $\beta = 1 - K_p/K_s$.

A similar procedure to that of Zhang is used to extend the model to binary mixtures (Zhang et al., 2008), the following equation can be obtained

$$\Delta\phi = \Delta\left(\frac{V_p}{V}\right) = \phi\left(\frac{1}{K} - \frac{1}{K_p}\right)(\Delta\overline{\sigma} - \Delta p) \tag{19}$$

Substituting Eqs. (16)–(18) into Eq. (19) yields

$$\Delta\phi = (\alpha - \phi)\left(\Delta\varepsilon_v + \frac{RT}{K_s}\sum_{j=1}^{2}\Delta C_j - \Delta\varepsilon_s\right) \tag{20}$$

Then, the porosity, ϕ, may be described as

$$\phi = \frac{1}{1+S}[(1+S_0)\phi_0 + \alpha(S - S_0)] \tag{21}$$

where $S = \varepsilon_v + \frac{RT}{K_s}\sum_{j=1}^{2} C_j - \varepsilon_s, S_0 = \varepsilon_{v0} + \frac{RT}{K_s}\sum_{j=1}^{2} C_{j0} - \varepsilon_{s0}$.

where ε_s is the total sorption-induced strain, as shown in Eq. (7) and ε_{s0} is the initial value.

Considering the cubic law relation (see Eq. (15)) between permeability and porosity of the porous media, we obtain

$$\frac{k}{k_0} = \left(\frac{1}{1+S}\left[(1+S_0) + \frac{\alpha}{\phi_0}(S - S_0)\right]\right)^3 \tag{22}$$

2.4. Binary gas transport

Mass transport in coal seam for CO_2 sequestration has been widely discussed and a number of different models have been used to quantify gas transport processes. In this paper, the binary transport of gas involves the gas flow through cleat and cracks, adsorption/desorption to coal matrix, advective transport and Fickian diffusion term through coal matrix to coal pores, so the mass balance equation can be expressed for a static medium incorporating these convective and dispersion modes of transport but involving the interchange between free and adsorbed gas as

$$\frac{\partial m_k}{\partial t} + \nabla\cdot(\vec{v}\cdot\rho_{gk}) + \nabla\cdot(-\vec{D}_k\cdot\nabla m_{fk}) = Q_{sk} \tag{23}$$

where m_k is the gas content including free-phase gas and absorbed gas. Expressions for the mass of free-phase gas, m_{fk}, and the mass of adsorbed gas, m_{sk}, may be defined for each component of the binary mixture as

$$m_{fk} = \phi\cdot C_k M_k \tag{24}$$

$$m_{sk} = (1-\phi)\cdot\rho_c\cdot\rho_{sg}\frac{V_{\infty k} b_k' C_k}{1 + C_1 b_1' + C_2 b_2'} \tag{25}$$

where $\vec{v}$ is the vector of convective velocity, determined by the injection gas concentration gradient, and can be expressed as

$$\vec{v} = -\frac{kRT}{\mu}\nabla C_2 \tag{26}$$

where ρ_{gk} is the gas density, ρ_{sg} is the gas density at standard conditions, ρ_c is coal density, M_k is the molar mass of component k, Q_{sk} is the gas source or sink, and $\vec{D}_k$ is the vector of hydrodynamic dispersion coefficient defined as

$$\vec{D}_k = \beta\cdot\vec{v} + D_{k0} \tag{27}$$

where D_{k0} is the coefficient of molecular diffusion of component k and β is the dynamic dispersivity. For simplicity, only the diagonal two components for dispersion coefficient are considered in this model.

Combining porosity Eq. (21) and Eqs. (23)–(27) yields the transport equations for CH_4 and CO_2,

$$\begin{aligned}&\left[\phi + \frac{\alpha-\phi}{1+S}C_1\left(\frac{RT}{K_s} - AA\right) + (1-\phi)\cdot\frac{\rho_c p_{at}}{RT}\cdot CC\right]\frac{\partial C_1}{\partial t}\\ &+ \left[\frac{\alpha-\phi}{1+S}C_1\left(\frac{RT}{K_s} - BB\right) - (1-\phi)\cdot\frac{\rho_c p_{at}}{RT}\cdot DD\right]\frac{\partial C_2}{\partial t} + \frac{\alpha-\phi}{1+S}C_1\frac{\partial\varepsilon_v}{\partial t}\\ &= \nabla\cdot[\vec{D}_1\phi\cdot\nabla C_1] - \nabla\cdot\left[-\frac{kRT}{\mu}C_1\cdot\nabla C_2\right]\end{aligned} \tag{28}$$

$$\begin{aligned}&\left[\phi + \frac{\alpha-\phi}{1+S}C_2\cdot\left(\frac{RT}{K_s} - BB\right) + (1-\phi)\cdot\frac{\rho_c p_{at}}{RT}\cdot C'C'\right]\frac{\partial C_2}{\partial t}\\ &+ \left[\frac{\alpha-\phi}{1+S}C_2\left(\frac{RT}{K_s} - AA\right) - (1-\phi)\cdot\frac{\rho_c p_{at}}{RT}\cdot D'D'\right]\frac{\partial C_1}{\partial t}\\ &+ \frac{\alpha-\phi}{1+S}C_2\frac{\partial\varepsilon_v}{\partial t} = \nabla\cdot[\vec{D}_2\phi\cdot\nabla C_2] - \nabla\cdot\left[-\frac{kRT}{\mu}C_2\cdot\nabla C_2\right]\end{aligned} \tag{29}$$

respectively.

where

$$CC = \frac{V_{\infty 1} b_1'(1 + b_2' C_2)}{(1 + C_1 b_1' + C_2 b_2')^2}, DD = \frac{V_{\infty 1} b_1' b_2' C_1}{(1 + C_1 b_1' + C_2 b_2')^2}, C'C' = \frac{V_{\infty 2} b_2'(1 + b_1' C_1)}{(1 + C_1 b_1' + C_2 b_2')^2}, D'D' = \frac{V_{\infty 2} b_1' b_2' C_2}{(1 + C_1 b_1' + C_2 b_2')^2}.$$

In the above equations, k is permeability and μ the dynamic viscosity of the gas. In Eq. (28), the summation of the first three terms (related to $\partial C_1/\partial t$) on the left side represent the resultant volume of gas released (or sequestered) from storage per unit change in the concentration of CH_4 (represented by C_1) and per unit volume of the reservoir. These three contributing components are, in order: (i) the volume of gas released (or sequestered) from the free-phase gas; (ii) the resultant volume of gas released (or sequestered) due to the cross-action between coal grain compaction and binary gas transport-induced shrinking or swelling in terms of the concentration change of C_1; and (iii) the volume of gas released (or sequestered) from the adsorbed-phase gas. The summation of the following two terms on the left side (related to $\partial C_2/\partial t$) represent the resultant volume of gas released (or sequestered) from storage per unit change in the concentration of CO_2, and per unit volume of the reservoir. These two contributing components are, in order: (i) the resultant volume of gas released (or sequestered) due to the cross-action between coal grain compaction and binary gas transport-induced shrinking or swelling in terms of the concentration change of C_2; and (ii) the volume of gas released (or sequestered) from the adsorbed-phase gas. The last term on the left side is the volume of gas released (or sequestered) due to coal bulk (skeletal) deformation. On the right-hand side, the first term represents the mass change rate due to dispersion while the second term represents the mass change rate due to flow. Similar explanations apply to Eq. (29) representing the transport of CO_2 (represented by C_2). Therefore, a set of governing equations for coupled coal matrix geomechanical deformation, binary gas flow and diffusion and gas absorption/desorption processes are

developed to define the issue of CO_2-ECBM and CO_2 geological sequestration.

2.5. Boundary and initial conditions

For the Navier-type Eq. (14), the displacement and stress conditions on the boundary are given as

$$u_i = \tilde{u}_i(t), \sigma_{ij} n_j = \tilde{F}_i(t) \text{ on } \partial\Omega \tag{30}$$

where $\tilde{u}_i$ and $\tilde{F}_i$ are the component of known displacement and stress on the boundary $\partial\Omega$, respectively. n_j is the directional cosine of the vector normal to the boundary.

For the gas convection and diffusion equations, if the concentration of the injected gas remains constant then the boundary condition is defined as

$$C = \tilde{C}(t) \text{ on } \partial\Omega \tag{31}$$

where $\tilde{C}(t)$ is the specified gas concentration on the boundary.

If the injection rate is a constant the boundary condition is defined as

$$\vec{n} \cdot (D_k \cdot \nabla C_k + \vec{v} C_k) = a_0 \tag{32}$$

where a_0 is the constant injection rate.

The above governing equations plus boundary and initial conditions are solved numerically in the following through a general PDE solver.

3. Mechanical response of coal

Eqs. (14), (28) and (29) describe coupled binary gas transport and coal deformation — this system is solved using a commercial PDE solver. In the following sections, we present results for the mechanical response of coal to CO_2 injection. A rectangular geometry is chosen in this study to represent coal–gas interaction assuming that the cleat porosity and coal seam properties are evenly distributed within the reservoir. Two simulations are presented in this paper to illustrate the effects of binary gas flow with diffusion and competitive adsorption on coal deformation. The first simulation verifies the coupled binary gas transport and coal deformation model through comparison experimental data (Mazumder et al., 2007), and the second explores the response of a prototypical in situ injection experiment at field scale.

3.1. Comparison with experimental data

In this example, a dry coal sample under a biaxial stress state is simulated to verify the validity of the FE model. The change in strain with time and the sweep efficiency of the produced gas against displaced volume are the model outputs compared with experimental measurements.

Table 1
Modeling parameters for the numerical simulation.

Parameter	Value
Poisson ratio of coal (ν)	0.34
Density of coal (ρ_c, kg/m^3)	1.25×10^3
Gas dynamic viscosity (μ, Pa. s)	1.84×10^{-5}
CH_4 Langmuir volume constant ($V_{\infty1}$, m^3/kg)	0.0256
CO_2 Langmuir volume constant ($V_{\infty2}$, m^3/kg)	0.0477
CH_4 Langmuir volumetric strain constant ($\varepsilon_{\infty1}$)	0.0128
CO_2 Langmuir volumetric strain constant ($\varepsilon_{\infty2}$)	0.0237
CH_4 Langmuir pressure constant (MPa)	2.07
CO_2 Langmuir pressure constant (MPa)	1.38
Initial porosity of coal (ϕ_0)	0.0423
Initial permeability of coal (k_0, m^2)	3.0×10^{-18}

3.1.1. Model description

The experimental sample is 334 mm long and 69.50 mm in diameter. The mean pore pressure is 4.3 MPa and the difference between the annular pressure and the pore pressure is 3.61 MPa, with CO_2 injected from the left side (6.0 ml/h) and flowing out from the right side. Because the sample is axially symmetric it can be approximated as a 2D model. The 2D plane strain model was taken along the axial direction, as shown in Fig. 1. Because this is a coupled model for coal deformation and binary gas transport, separate boundary and initial conditions are applied to each model. For the coal deformation model, the left side and bottom boundaries are constrained in the horizontal and vertical directions, respectively; the overburden stress on the upper face is 7.91 MPa and the right side is unconstrained. The coal property parameters are listed in Table 1 and are selected from the experimental results (Mazumder et al., 2008; Shi et al., 2008) and supplementary sources (Shi and Durucan, 2004; Robertson and Christiansen, 2005; Raharjo et al., 2007). For the binary gas transport model, the coal is initially saturated with CH_4 at a pressure of 4.3 MPa with injection of CO_2 at constant rate.

3.1.2. History matching results and discussion

The comparison between modeling results and experimental data is shown in Fig. 2. As shown in Fig. 2(a) a delay in swelling response relative to the onset of CO_2 injection was observed, due to the delay in injected CO_2 arriving within the sample and acting and therefore related swelling induced volume change. Fig. 2(a) also shows that the simulation results match the experimental curve reasonably well, and the strain change characteristic is very close to the trendline of the experimental data. The largest error is at the initial stage, but after two days the model and data trendline match with a mean error of only 3.2%.

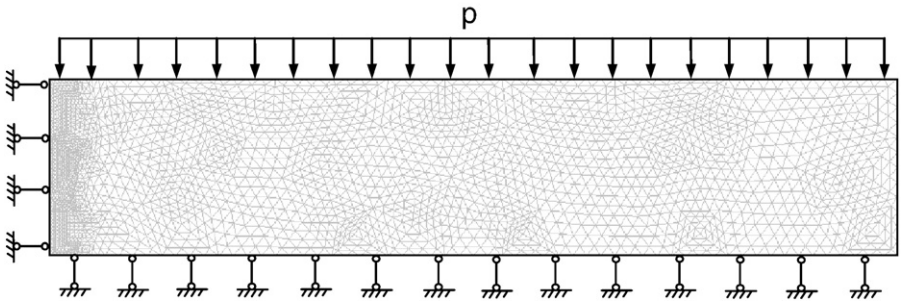

Fig. 1. Schematic of the simulation model built to represent experimental conditions (Mazumder et al., 2008).

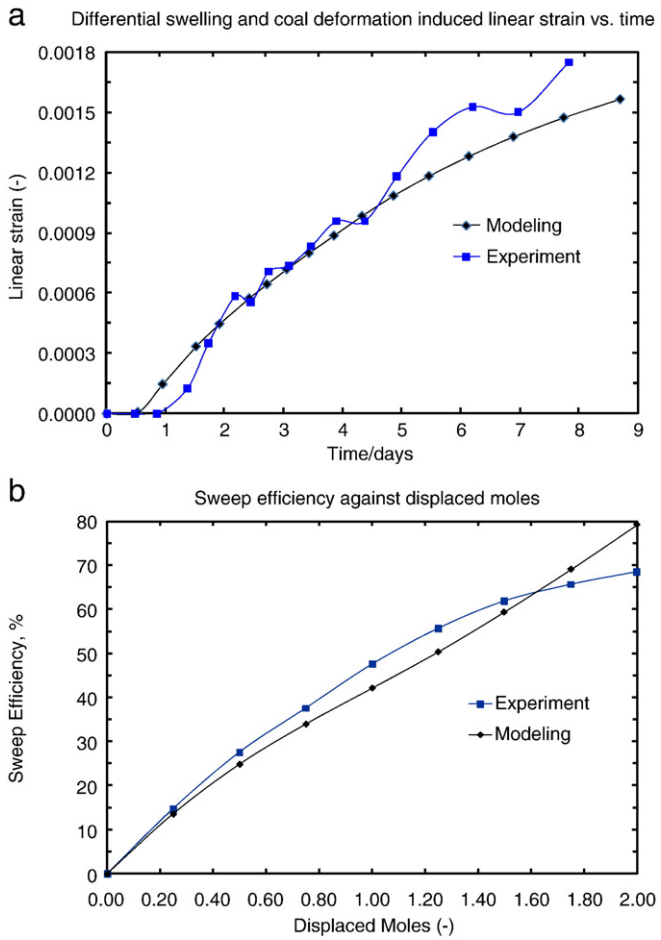

Fig. 2. Comparison between modeling results and experimental data.

The relation between the change in sweeping efficiency and the displaced volume is shown in Fig. 2(b). Sweep efficiency and displaced volume used in this paper are defined as follows:

$$Sweep\ efficiency = \frac{moles\ of\ CH_4\ produced \times 100\%}{moles\ of\ CH_4\ initially\ in\ place}$$

$$Displaced\ volume = \frac{moles\ of\ CO_2\ injected}{moles\ of\ CH_4\ initially\ in\ place}$$

It can be seen from Fig. 2(b) that the simulation results match experimental data reasonably well, even though the trend for the modeling curve is more linear than the testing result. The largest error occurs when the displaced volume is equal to two, with an error of 15.6%; that is because in our simulation model, the driving force for CH_4 displacement is from the concentration gradient of CO_2. Theoretically, bigger CO_2 concentration gradient accompanies quicker CH_4 displacement. In the experiment, in the final stage of displacement, the influence of convective process on CH_4 concentration change could be slight and its change may mainly be controlled by diffusion process. In other words, the sweep efficiency is overestimated a little bit in our simulation model in the final stage. Therefore, with CO_2 injection, we can see that the sweep efficiency is increasing even faster, and big difference with experiment is caused. The mean error value for the whole curve is 4.0%.

The successful match between modeled results and experimental data has demonstrated the validity of the FE model. In the following section, the model is used to predict the performance of CO_2-ECBM technology implementation in field scale.

3.2. Field scale response

A field scale model incorporating a five-spot well pattern is used to simulate the performance of CO_2-ECBM under in-situ conditions. Input parameters for this simulation are identical to the parameters used in Section 3.1. The influence of some controlling parameters, including the Young modulus and Poisson ratio of the coal, the initial coal permeability and gas sorption-induced strain capacity on the gas sorption rate and capacity (gas mole fraction), evolution of permeability and change in CO_2 injectivity are investigated in detail. The evolution of CO_2 injectivity is further discussed as this has crucial importance on the successful implementation of the CO_2-ECBM projects.

3.2.1. Model description

The five-spot well pattern model geometry of 100 m by 100 m is shown in Fig. 3 with the CO_2 injection well centered within the block and with the four CH_4 recovery wells located at the vertices. For the coal deformation model, all four sides are confined in the normal direction while the production and injection wells are unconfined. For the binary gas transport model, the coal is saturated initially with CH_4 and the initial pressure is 4.3 MPa. The Neumann boundary conditions $(\vec{n}\cdot(\vec{D}_k\cdot\nabla C_k) = 0)$ are specified at the four production wells, and the constant injection pressure condition is specified at the injection well.

3.2.2. Simulation strategies

In order to investigate the mechanical response of the coal seam to CO_2 injection, four sets of simulations were conducted to investigate the effects of coal mechanical properties on the gas injection performance under different coal matrix Young moduli and Poisson ratios; to calculate the influence of initial permeabilities on the implementation of CO_2-ECBM technology under different values; and to investigate the influence of gas components on CO_2 injection efficiency and CH_4 production under three different gas swelling strain constants. The detailed simulation strategies are shown in Table 2.

4. Results and discussion

A(25,25) is the analysis point, as shown in Fig. 3. The model results are presented for each simulation case in terms of the evolution of the

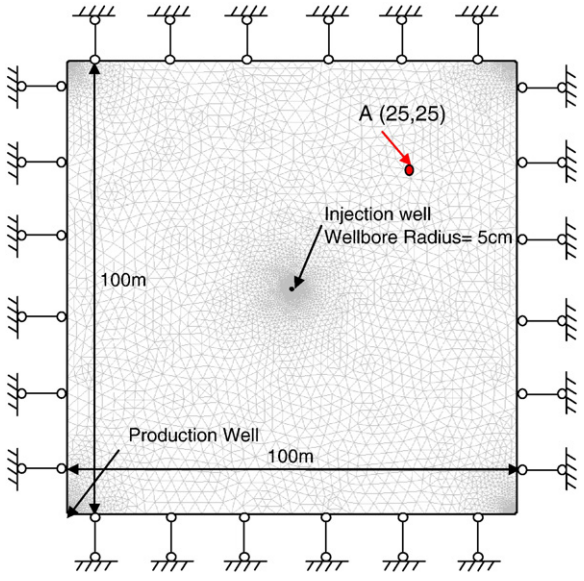

Fig. 3. Field-scale model: five-spot well pattern model with the CO_2 injection well centered and the four CH_4 recovery wells located at the vertices.

Table 2
Simulation strategies.

Case 1	Impact of Young moduli on the resulting response $E=2.71$; 4.07; 5.42 MPa
Case 2	Impact of Poisson ratios on the resulting response $\mu=0.20$; 0.34; 0.40
Case 3	Impact of initial permeabilities on the resulting response $k_0=3\times10^{-16}$; 3×10^{-17}; 3×10^{-18}m^2
Case 4	Impact of gas swelling strain constants on the resulting response $\varepsilon_{\infty 2}=0.0119$; 0.0237; 0.0474

permeability ratio, the mole fractions of CH_4 and CO_2, CO_2 injection rate and the pore pressure distribution along the diagonal line between the production well and the injection well at $t=100$ d. These results are shown in Figs. 4–8.

4.1. Impact of coal mechanical properties

Fig. 4(a) shows that a smaller Young modulus results in a less reduction in coal permeability as pore pressure increases. When $E=2.71$ GPa, initially, the permeability decreases with gas injection until permeability ratio reduces to 0.88 (pore pressure is about 11 MPa), followed a rebound in permeability with CO_2 injection. The turning point marks the transition from the dominance of the gas sorption-induced permeability change to the dominance of the effective stress change induced permeability change. However, the turning points were not observed for moduli of $E=4.07$ GPa and 5.42 GPa where the permeability decreases monotonically with CO_2 injection for the whole injection process. This illustrates that sorption-induced permeability change plays a more significant role than the influence of effective stress within this range of pore pressure. As shown in Fig. 4(b), the peak values of the gas injection rate are similarly regulated by the magnitudes of coal moduli: a lower coal modulus results in a larger CO_2 injection rate since permeability remains elevated even as gas pressures increase throughout the reservoir.

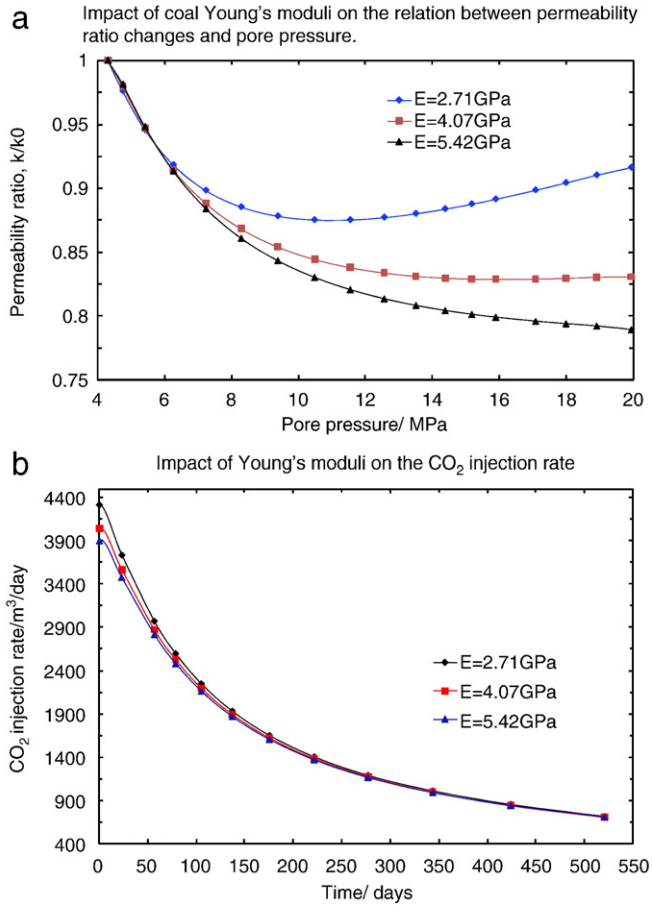

Fig. 4. Sensitivity of the model to Young's modulus.

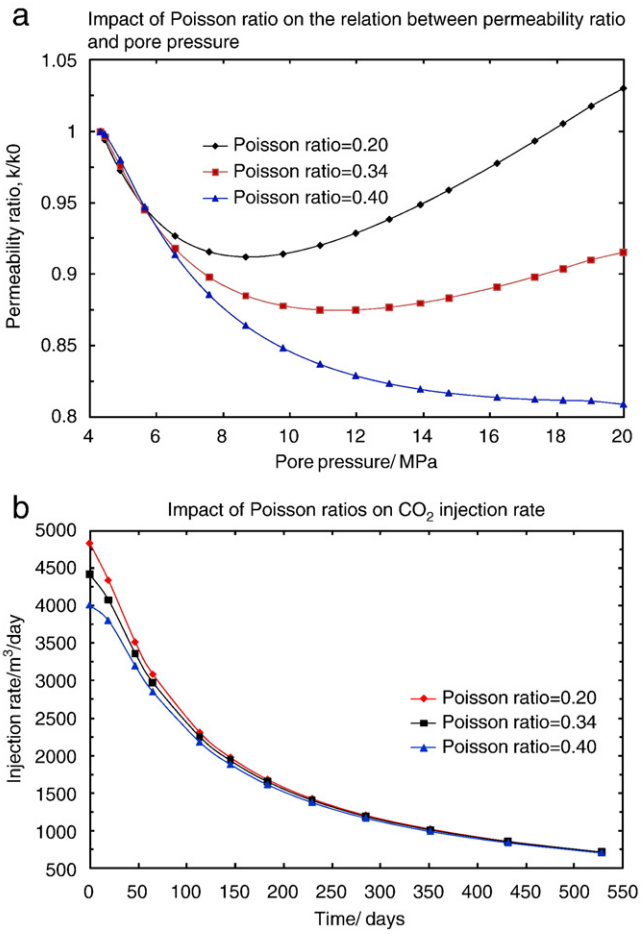

Fig. 5. Sensitivity of the model to Poisson ratio.

Fig. 5(a) shows that the magnitude of the Poisson ratio also has a significant impact on the permeability. When $\mu=0.20$, the permeability decreases from the initial 1.0 to 0.92, and then rebounds to 1.04 at the end of gas injection. A similar pattern is observed for the case of $\mu=0.34$. The turning point from decrease to increase marks the transition from the dominance of the gas sorption-induced permeability change to the dominance of the effective stress induced permeability change. However, the turning point was not observed for the case of $\mu=0.40$. In this case, the permeability decreases monotonically with CO_2 injection for the whole injection process. Fig. 5(b) shows the impact of Poisson ratios on the injection rate, again reflecting the influence of permeability change modulated by Poisson ratio.

4.2. Impact of initial permeability

Fig. 6 shows the impact of the initial permeability on the evolutions of permeability ratio, gas concentration, injection rate, and pore pressure. When the gas pressure increases, CO_2 and CH_4 advection changes the composition of gas components in the coal matrix. The increase of pore pressure results in a decrease of

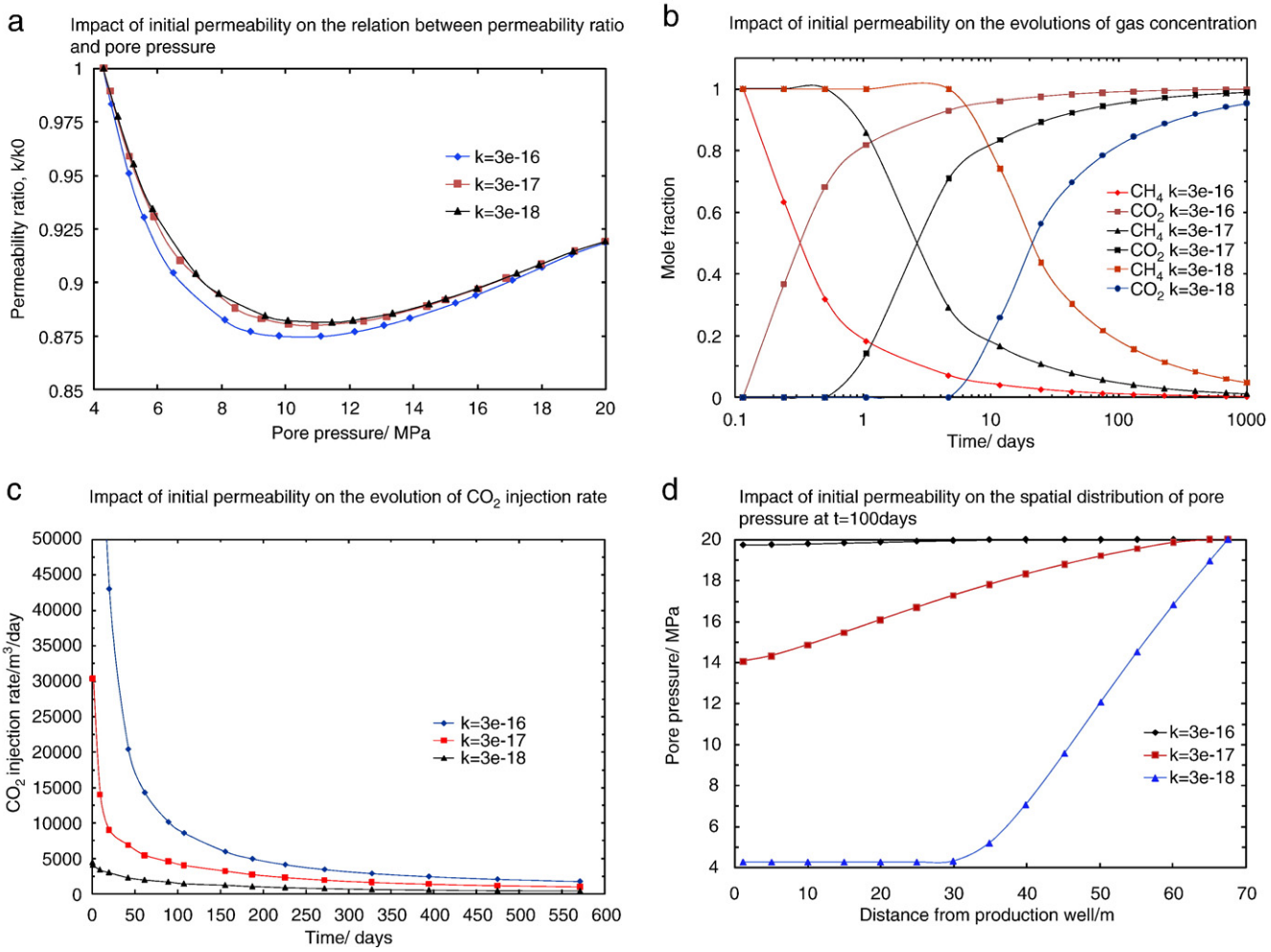

Fig. 6. Sensitivity of the model to initial permeability.

effective stress. The reduction in effective stress enhances the coal permeability. In contrast, the binary gas diffusion induced differential swelling of the coal matrix reduces the cleat apertures and decreases the permeability. The net change in permeability accompanying gas diffusion is controlled competitively by the influence of effective stresses and differential matrix swelling. Therefore the impact of the initial permeability is minimal as shown in Fig. 6(a). The transport of gases is controlled both by the dispersion and the convection processes. Because the coal permeability is controlled both by the initial permeability and by the change ratio, the initial permeability has a significant impact on the movement of the gas diffusion front. As shown in Fig. 6(b), this movement is inversely proportional to the initial permeability. Under constant injection pressure, the injection rate is primarily controlled by the coal permeability. The coal permeability is a summation of the initial permeability and the permeability change regulated by the influence of effective stresses and differential matrix swelling. As shown in Fig. 6(a), the permeability change is from 0 to $0.88k_0$ for all three cases. This means that the gas injection rate is primarily controlled by the initial permeability, as shown in Fig. 6(c). Under the constant injection pressure, the CO_2–CH_4 displacement front is primarily by convection together with a small effect from CO_2 and CH_4 dispersion. Therefore, the front displaces at a velocity proportional to the initial permeability as shown in Fig. 6(b). The pore pressure in the coal is close to the injection pressure behind the front. As shown in Fig. 6(d), the pore pressure is almost constant when the initial permeability is equal to $3\times10^{-16}m^2$. This is because the displacement front has reached the outside boundary. For the other two cases with smaller permeabilities, the pore pressures are significant less that the injection pressure because the displacement fronts has not reached the outside boundary.

4.3. Impact of gas swelling strain constants

The net change in permeability accompanying binary gas diffusion is controlled competitively by the influence of effective stresses and differential matrix swelling. In this simulation, three different magnitudes of the gas swelling strain constant were used to alter the balance between the sorption-induced permeability change and the effective stress-induced permeability change. Modeling results are shown in Fig. 7.

The model of with the strain constant reduced by one half (case 1) is to simulate the binary gas injection of an N_2/CO_2 mixture, maybe representing direct injection of flue gas, as a method to dramatically increase gas injectivity but with a lower CO_2 concentration per unit mass of gas injected (e.g. Durucan and Shi, 2008). Conversely the model with twice strain constant (case 3) is to represent the affinity to other coals of different rank with much larger gas swelling strain constants (Robertson and Christiansen, 2005; Mazumder et al., 2008; Shi et al., 2008).

The impact of the gas swelling strain constant on the permeability change is shown in Fig. 7(a). For case 1, the influence of effective stress

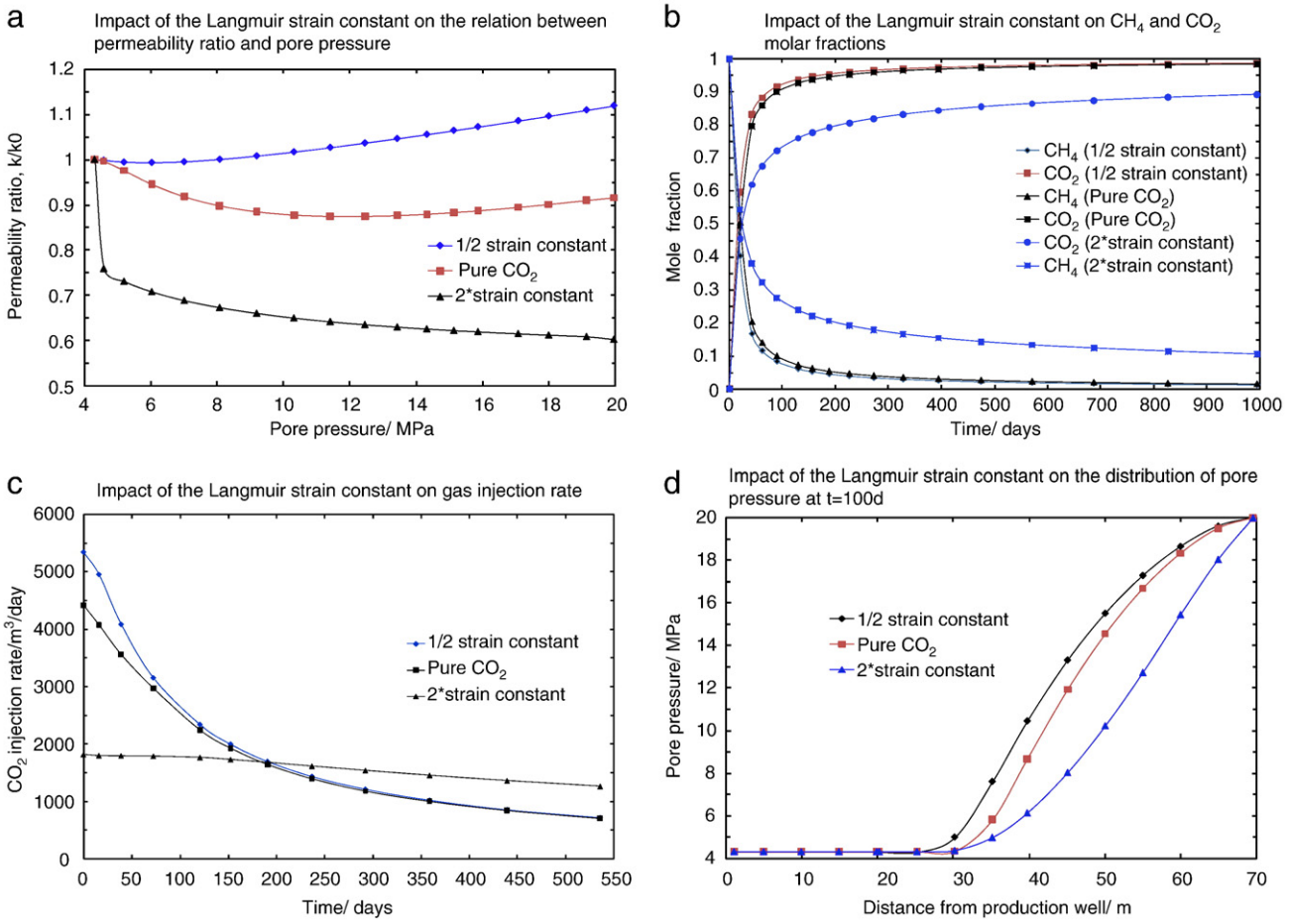

Fig. 7. Sensitivity of the model to the injection gas Langmuir strain constants.

change on permeability is dominant, while the impact of the sorption-induced permeability change is secondary; for the pure CO_2 model, the gas sorption-induced permeability change is dominant over the effective stress change induced permeability in the initial stages; as injection proceeds, the mechanical influence takes over the dominant role. However, for case 3, the gas sorption-induced permeability change always plays a dominant role during CO_2 injection within this range of pore pressure.

Fig. 7(b) shows the evolution of gas mole fractions at the reference location under different gas swelling strain constants. For case 1 and the pure CO_2 models, gas mole fractions reach steady values within about 200 days, but for case 3, this percentage is much higher (about 20%) and it still needs long time to complete CH_4 displacement. These observations illustrate that the gas swelling strain constant affects both the gas dispersion and the gas convection.

Fig. 7(c) shows the impact of the gas swelling strain constant on the gas injection rate. For case 1 and for pure CO_2 models, the permeability changes gradually from the initial value to decrease to increase. However, an almost instant 25% reduction takes place for case 3 model. These changes in permeability are consistent with the changes in injection rate.

Fig. 7(d) shows the impact of the gas swelling strain constant on the distribution of pore pressure.

For all three cases, the displacement front has not reached the outside boundary. This is why the pore pressures are much smaller than the outside boundary pressure (or the injection pressure).

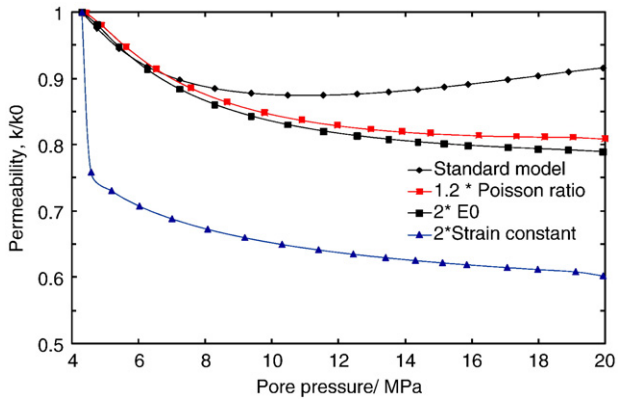

Fig. 8. Sensitivity of the model to the reservoir and injection gas parameters.

4.4. Comparison of impacts

The net change in permeability accompanying binary gas diffusion is controlled competitively by the influence of effective stresses and differential matrix swelling. The balance between these two influences can be altered either by changing mechanical parameters (Young's modulus and Poisson ratio) or by changing the sorption properties such as the gas swelling strain constant. Their relative importance is illustrated in Fig. 8. This graph shows that the coal permeability is more sensitive to the gas sorption properties than coal mechanical parameters.

5. Conclusions

A fully coupled coal deformation, binary gas flow and diffusion and gas absorption/desorption finite element (FE) model is developed to achieve a better understanding of the CO_2-ECBM recovery mechanisms. A dry coal sample under the triaxial stress state was simulated and the simulation results successfully match the experimental data. Following this verification, a field scale model was used to predict the performance of CO_2-ECBM technology implementation under in-situ conditions.

Modeling results indicate that the net change in coal permeability accompanying binary gas dispersion is controlled competitively by the influence of effective stresses and differential matrix swelling. The balance between these two influences can be altered either by changing mechanical parameters (Young's modulus and Poisson ratio) or by changing the coal sorption properties such as the swelling strain. The impact of gas sorption induced deformation on coal permeability increases with the magnitudes of coal Young's modulus or Poisson ratio, and with the magnitudes of the gas swelling strain constant.

Acknowldgements

This work was supported by WA:ERA, the Western Australia CSIRO-University Postgraduate Research Scholarship, National Research Flagship Energy Transformed Top-up Scholarship, and by NIOSH under contract 200-2008-25702. These supports are gratefully acknowledged.

References

Busch, A., Gensterblum, Y., Krooss, B.M., Littke, R., 2004. Methane and carbon dioxide adsorption–diffusion experiments on coal: upscaling and modeling. International Journal of Coal Geology 60, 151–168.

Butler, J.A.V., Ockrent, C., 1930. Studies in electrocapillarity. Part III. The surface tensions of solutions containing two surface-active solutes. The Journal of Physical Chemistry 34, 2841–2859.

Chaback, J.J., Morgan, W.D., Yee, D., 1996. Sorption of nitrogen, methane, carbon dioxide and their mixtures on bituminous coals at in-situ conditions. Fluid Phase Equilibria 117, 289–296.

Charrièrea, D., Pokryszk, Z., Behra, P., (Article in press). Effect of pressure and temperature on diffusion of CO_2 and CH_4 into coal from the Lorraine basin (France). International Journal of Coal Geology. doi:10.1016/j.coal.2009.03.007.

Chikatamarla, L., Cui, X., Bustin, R.M., 2004. Implications of volumetric swelling/shrinkage of coal in sequestration of acid gases. International Coalbed Methane Symposium Proceedings, Tuscaloosa, Alabama, paper 0435.

Connell, L.D., Detournay, C., 2009. Coupled flow and geomechanical processes during enhanced coal seam methane recovery through CO_2 sequestration. International Journal of Coal Geology 77, 222–233.

Cui, X.J., Bustin, R.M., 2005. Volumetric strain associated with methane desorption and its impact on coalbed gas production from deep coal seams. AAPG Bulletin 89 (9), 1181–1202.

Day, S., Fry, R., Sakurovs, R., 2008. Swelling of Australian coals in supercritical CO_2. International Journal of Coal Geology 74 (1), 41–52.

Detournay, E., Cheng, A.H.D., 1993. Fundamental of poroelasticity. In: Fairhurst, C. (Ed.), Comprehensive Rock Engineering, vol. II. Pergamon, Oxford, pp. 113–171.

Do, D.D., 1998. Adsorption analysis: equilibria and kinetics. Imperial College Press, London.

Dubinin, M.M., 1966. In: WalkerJr. Jr., P.L. (Ed.), Chemistry and Physics of Carbon, vol. 2. Marcel Dekker, New York.

Durucan, S., Shi, J.-Q., 2008. Improving the CO_2 well injectivity and enhanced coalbed methane production performance in coal seams. International Journal of Coal Geology 77, 214–221.

Fathi, E., Akkutlu, I.Y., 2008. Counter-diffusion and competitive adsorption effects during CO_2 injection and coalbed methane production. SPE-Society of Petroleum Engineers 115482.

Fathi, E., Akkutlu, I.Y., 2009. Matrix heterogeneity effects on gas transport and adsorption in coalbed and shale gas reservoirs. Transport in Porous Media 80, 281–304.

Fokker, P.A., van der Meer, L.G.H., 2004. The injectivity of coalbed CO_2 injection wells. Energy 29, 1423–1429.

Gray, I., 1992. Reservoir engineering in coal seams: Part 1 — the physical process of gas storage and movement in coal seams. Coalbed methane: Society of Petroleum Engineers, Reprint Series, vol. 35, pp. 7–13.

Gunter, W.D., Gentzis, T., Rottenfuser, B.A., Richardson, R.J.H., 1997. Deep coalbed methane in Alberta, Canada: a fuel resource with the potential of zero greenhouse gas emissions. Energy Conversion Management 38, 217–222.

Hall, F.E., Zou, C.H., Gasem, K.A.M., Robinson, R.L., Yee, D., 1994. Adsorption of pure methane, nitrogen, and carbon dioxide and their binary mixtures on wet Fruitland coal. SPE 29194-MS.

IPCC, 2005. IPCC special report on carbon dioxide capture and storage. Cambridge University Press, UK.

Karacan, C.O., 2007. Swelling-induced volumetric strains internal to a stressed coal associated with CO_2 sorption. International Journal of Coal Geology 72, 209–220.

King, G.R., 1990. Material balance techniques for coal seam and devonian shale gas reservoirs. SPE 20730.

Korre, A., Shi, J.-Q., Imrie, C., Grattoni, C., Durucan, S., 2007. Coalbed methane reservoir data and simulator parameter uncertainty modelling for CO_2 storage performance assessment. International Journal of Greenhouse Gas Control 1 (4), 492–501.

Krooss, B.M., Van Bergen, F., Gensterblum, Y., Siemons, N., Pagnier, H.J.M., David, P., 2002. High-pressure methane and carbon dioxide adsorption on dry and moisture-equilibrated Pennsylvanian coals. International Journal of Coal Geology 51 (2), 69–92.

Kuuskraa, V.A., Boyer, J.N., 1992. Coalbed gas 1—hunt for quality basins goes abroad. Oil and Gas Journal, OGJ Special—Unconventional Gas Development 5, 49–54.

Langmuir, I., 1916. The constitution and fundamental properties of solids and liquids. Part I. solids. Journal of the American Chemical Society 38, 2221–2295.

Larsen, J.W., 2003. The effects of dissolved CO_2 on coal structure and properties. International Journal of Coal Geology 57 (1), 63–70.

Levine, J.R., 1996. Model study of the influence of matrix shrinkage on absolute permeability of coal bed reservoirs. Geological Society of London, Special Publication 109, 197–212.

Mazumder, S., Wolf, K.-H., 2007. Differential swelling and permeability change of coal in response to CO_2 injection for ECBM. International Journal of Coal Geology 74, 123–138.

Mazumder, S., Wolf, K-H.A.A, Bruining, H., 2005. The relationship between coal macromolecular structure and its swelling. Proceedings International RECOPOL workshop Szcyrk (Poland).

Mazumder, S., Wolf, K.H.A.A., Van Hemert, P., Busch, A., 2008. Laboratory experiments on environmental friendly means to improve coalbed methane production by carbon dioxide/flue gas injection. Transport in Porous Media 75, 63–92.

Moffat, D.H., Weale, K.E., 1955. Sorption by coal of methane at high pressure. Fuel 34, 449–462.

Palmer, I., 2009. Permeability changes in coal: analytical modeling. International Journal of Coal Geology 77, 119–126.

Palmer, I., Mansoori, J., 1996. How permeability depends on stress and pore pressure in coalbeds: a new model. SPE-52607.

Pan, Z.J., Connell, L.D., 2009. Comparison of adsorption models in reservoir simulation of enhanced coalbed methane recovery and CO_2 sequestration in coal. International Journal of Greenhouse Gas Control 3, 77–89.

Pekot, L.J., Reeves, S.R., 2002. Modeling the effects of matrix shrinkage and differential swelling on coalbed methane recovery and carbon sequestration. U.S. Department of Energy DE-FC26-00NT40924.

Pone, J.D.N., Hile, M., Halleck, P.M., Mathews, J.P., 2008. Three-dimensional carbon dioxide-induced strain distribution within a confined bituminous coal. International Journal of Coal Geology 77, 103–108.

Prusty, B.K., 2007. Sorption of methane and CO_2 for enhanced coalbed methane recovery and carbon dioxide sequestration. Journal of Natural Gas Chemistry 17, 29–38.

Raharjo, R.D., Freeman, B.D., Paul, D.R., Sarti, G.C., Sanders, E.S., 2007. Pure and mixed gas CH_4 and n-C_4H_{10} permeability and diffusivity in poly (dimethylsiloxane). Journal of Membrane Science 306, 75–92.

Robertson, E.P., Christiansen, R.L., 2005. Measurement of sorption-induced strain. International Coalbed Methane Symposium, University of Alabama, Tuscaloosa. Paper 0532.

Robertson, E.P., Christiansen, R.L., 2007. Modeling laboratory permeability in coal using sorption-induced-strain data. SPE Reservoir Evaluation and Engineering 10 (3), 260–269.

Seidle, J.P., Huitt, L.G., 1995. Experimental measurement of coal matrix shrinkage due to gas desorption and implications for cleat permeability increases. SPE-30010-MS.

Shi, J.-Q., Durucan, S., 2004. A numerical simulation study of the Allison unit CO_2 -ECBM pilot: the impact of matrix shrinkage and swelling on ECBM production and CO_2 injectivity. Proceedings of 7th International Conference on Greenhouse Gas Control Technologies.

Shi, J.-Q., Durucan, S., 2005. A model for changes in coalbed permeability during primary and enhanced methane recovery. SPE Reservoir Evaluation and Engineering 8 (4), 291–299.

Shi, J.-Q., Durucan, S., 2008. Modeling of mixed-gas adsorption and diffusion in coalbed reservoirs. SPE 114197.

Shi, J.-Q., Mazumder, S., Wolf, K.-H., Durucan, S., 2008. Competitive methane desorption by supercritical CO_2 injection in coal. Transport in Porous Media 75, 35–54.

Siemons, N., Busch, A., 2007. Measurement and interpretation of supercritical CO_2 sorption on various coals. International Journal of Coal Geology 69 (4), 229–242.

Stauffer, P.H., Viswanathan, H.S., Pawar, R.J., Guthrie, G.D., 2009. A system model for geologic sequestration of carbon dioxide. Environmental Science & Technology 43 (3), 565–570.

Stevens, S.H., Kuuskraa, V.A., Spector, D., Riemer, P., 1999. CO_2 sequestration in deep coal seams: pilot results and worldwide potential. Proceedings of the 4th International Conference on Greenhouse Gas Control Technologies, Interlake, Switzerland, pp. 175–180.

Wang, G.X., Massarottoa, P., Rudolpha, V., 2009. An improved permeability model of coal for coalbed methane recovery and CO_2 geosequestration. International Journal of Coal Geology 77, 127–136.

Wei, X.R., Wang, G.X., Massarotto, P., Golding, S.D., Rudolph, V., 2007. Numerical simulation of multicomponent gas diffusion and flow in coals for CO_2 enhanced coalbed methane recovery. Chemical Engineering Science 62 (16), 4193–4203.

White, C.M., Smith, D.H., Jones, K.L., et al., 2005. Sequestration of carbon dioxide in coal with enhanced coalbed methane recovery: a review. Energy Fuels 19 (3), 659–724.

Yi, J., Akkutlu, I.Y., Deutsch, C.V., 2008. Gas transport in bidisperse coal particles: investigation for an effective diffusion coefficient in coalbeds. Journal of Canadian Petroleum Technology 47 (10), 20–26.

Zhang, H.B., Liu, J., Elsworth, D., 2008. How sorption-induced matrix deformation affects gas flow in coal seams: a new FE model. International Journal of Rock Mechanics and Mining Sciences 45 (8), 1226–1236.